Tetrahedron 73 (2017) 472–480

Contents lists available at ScienceDirect

Tetrahedron

journal homepage: www.elsevier.com/locate/tet

Thiophene ring-fragmentation reactions: Principles and scale-up towards NLO materials

Daniel Lumpi [a, *], Johannes Steindl [a], Sebastian Steiner [a], Victor Carl [a], Paul Kautny [a], Michael Schön [a], Florian Glöcklhofer [a], Brigitte Holzer [a], Berthold Stöger [b], Ernst Horkel [a], Christian Hametner [a], Georg Reider [c], Marko D. Mihovilovic [a], Johannes Fröhlich [a]

[a] Institute of Applied Synthetic Chemistry, TU Wien, Getreidemarkt 9/163, A-1060 Vienna, Austria
[b] Institute of Chemical Technologies and Analytics, TU Wien, Getreidemarkt 9/164-SC, A-1060 Vienna, Austria
[c] Photonics Institute, TU Wien, Gußhausstraße 27-29, A-1040 Vienna, Austria

ARTICLE INFO

Article history:
Received 26 September 2016
Received in revised form
10 December 2016
Accepted 12 December 2016
Available online 18 December 2016

Keywords:
Thiophene ring-opening
Reaction mechanism
Reaction kinetics
Inline monitoring
Second harmonic generation

ABSTRACT

A systematic study on the thiophene ring-fragmentation (TRF) reaction, yielding the Z-isomer of ene-yne type compounds, is presented. The investigations focus on the origins and pathways of potential side-reactions, resulting in an advanced synthetic protocol featuring enhanced selectivity and efficiency. The fragmentation threshold temperatures as well as reaction kinetics have been investigated utilizing inline infrared spectroscopy revealing unexpected results particularly concerning the reaction order (zero-order process). With regard to safety, selectivity, and up-scaling a flow-chemistry procedure for the TRF reaction has been developed. Finally, the technological relevance of the ene-yne structural motif is extended by a new design concept for NLO-chromophores showing the highest second harmonic generation efficiencies reported for these scaffolds.

1. Introduction

The base induced ring-opening reaction of heterocycles is a well-established methodology in organic chemistry.[1] In particular, the organo-metal intermediated ring-fragmentation of thiophene derivatives, leading to “ene-yne” type compounds, is one of the best-studied ring-opening reactions.[1–3] Early observations of the formation of “unsaturated aliphatic products” from 3-thienyl-lithium date back to 1962,[4] however, the mechanism has not been understood at that time. The first report on controlled ring-fragmentation was given by Gronowitz et al. in 1969 on the selenophene structure.[5] These findings were followed by publications of S. Gronowitz et al.[6] and K. Jakobsen[7] demonstrating thiophene ring-opening reactions; similar studies on benzo[*b*]thiophene were presented by B. Iddon et al.[8] Recent extensions of the strategy represent double-sided ring-opened species *via* a tandem fragmentation process.[9–11]

Thiophene ring-fragmentations (TRF) (Scheme 1) proceed with remarkable stereoselectivity yielding *Z*-isomers, selectively[1–3,5–11]; alternative approaches to synthesize these scaffolds typically suffer from poor regio- or/and stereoselectivity.[1] Driven by the broad variety of potential applications, intense research in the development of stereoselective approaches *via* e.g. carbo- or hydrothiolation, in order to obtain *Z*-organylthioenynes but also vinyl sulfides,[12–17] has been reported.

The scope of possible modifications, functionalizations (e.g. cycloaddition, Sonogashira-coupling, Michael-addition, nucleophilic substitution, oxidation) and applications of TRF-products was demonstrated to be widespread.[18] Another important factor for applications, e.g. in materials science, is the potential to selectively oxidize the alkylthio group.[18,19] This strategy enables to convert the +M- (alkylthio) directly into a −M-substituent (sulfoxide or sulfone), thus significantly influencing electronic properties.[20]

Moreover, ene-yne substructures are found in natural products (e.g. Anthemis species)[21–23] and, thus, represent attractive building blocks for total synthesis. Organylthioenynes are also useful synthons in organic synthesis, as these scaffolds can be utilized as precursors to enediynes and other functionalized olefins.[14] Vinyl sulfides are widely applied in organic synthesis as versatile intermediates[12] and were identified in several biologically active

* Corresponding author.
E-mail address: daniel.lumpi@tuwien.ac.at (D. Lumpi).

http://dx.doi.org/10.1016/j.tet.2016.12.025
0040-4020/

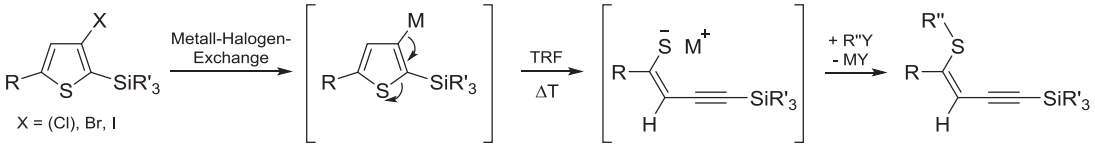

Scheme 1. Generally accepted reaction mechanism of thiophene ring-fragmentation.

molecules.[12–14,24–26] In particular, aromatic vinyl-sulfide derivatives are found in various pharmaceutically active drugs against important diseases such as Alzheimer's, Parkinson's, diabetes, AIDS, and cancer.[14,27,28] For potential pharmaceutical applications the selectivity of the synthetic approach with respect to double bond geometry is an important issue.

Recently, our group has reported on ene-yne derived nonlinear optical (NLO) materials capable of second harmonic (SH) generation.[29–31] Direct functionalization of TRF-products *via* copper(I)-catalyzed azide-alkyne cycloaddition (CuAAC)[32,33] applying phenylazide yielded NLO materials featuring twice the SH-efficiency of potassium dihydrogen phosphate (KH_2PO_4 - KDP).[30] Furthermore, replacing sulfur by selenium resulted in 20-fold higher SH-efficiency due to an increased electron density leading to enhanced hyperpolarizibility.[31]

Applications in the field of materials science in particular necessitate efficient and reliable synthetic access to TRF-products. Here, we present a systematic study on the thiophene ring-opening approach focusing on origins and pathways of potential side reactions. As a result, an advanced procedure leading to significantly improved *Z*-selectivity and efficiency is being developed. We investigated the reaction kinetics of the TRF, applying inline monitoring *via* infrared spectroscopy and implemented flow chemistry for safe and convenient scalability of the process. In addition, the development of an improved design concept for NLO-chromophores, yielding the highest SH-generation efficiencies reported for TRF-based products up to date, underlines the technological relevance of ene-yne compounds.

2. Results and discussion

2.1. Thiophene ring-fragmentation

In the course of our research on NLO materials, utilizing (*Z*)-trimethyl(4-(methylthio)pent-3-en-1-inyl)silane (**3a**, Scheme 2) as an ene-yne scaffold, deviations from the synthetic protocol[30] (e.g. loss of inert atmosphere) resulted in an unexpected *E*/*Z*-isomerization of **3a** toward the *E*-species **3f** (typically in the range of 1–5%). For this reason, the impact of the reaction components on the isomerization was evaluated. It could be shown that neither the used dry solvent (Et_2O), the reactants (**2a**, *n*-BuLi, MeI) nor the organic by-products (*n*-BuBr) are associated with this process. However, the addition of LiI, which is formed during quenching of the TRF reaction using MeI, results in an isomerization of **3a**. By evaluating various salts containing Li^+- or I^--ions (LiCl, LiBr, $LiClO_4$, LiI, NaI, KI and TBAI – see Supplementary Data) it was established that the iodide anion is responsible for this side-reaction. Interestingly, this reaction showed enhanced rates in the presence of oxygen; argon atmosphere significantly limits this effect.

From these experiments we concluded that the formation of elemental iodine (I_2), even if only present in traces, is the origin of the formation of the *E*-species. This I_2-induced process of double bond isomerization is well-described in literature.[34] Indeed, a control experiment revealed that the addition of I_2 (1 mol%) induces this reaction (Fig. 1); full exclusion of light suppresses the isomerization.

To further quantify this side reaction, **3a** and the corresponding *E*-isomer **3f** were subjected to UV-light assisted isomerization experiments. The reactions were carried out in standard NMR tubes using an I_2 solution in $CDCl_3$ at concentrations of 1.0 mol% and a standard light source.[35] The results for 1.0 mol% I_2 are illustrated in Fig. 1. The experiment yielded the same *E*/*Z*-ratio starting from both, the pure *Z*- and *E*-isomer, indicating that complete equilibration is reached during the I_2-induced isomerization. Additional experiments using 10.0 mol% I_2 and starting material **3a** revealed that an equilibrium state between the *Z*- and *E*-isomer is already reached within 15 s of light irradiation.

The equilibrium state consists of 16% **3a** (*Z*-isomer) compared to an 84% **3f** (*E*-isomer), corresponding to the thermodynamic energy level difference between the *Z*- and the *E*-isomer as indicated by DFT calculations. This fact clearly points out the importance of the TRF approach to obtain the thermodynamically less favored isomer. Moreover, the strategy potentially allows obtaining the corresponding *E*-structure in good yields. Indeed, repeating this experiment on preparative scale (using a 1.0 mol% I_2 solution) resulted in 76% of pure (*E*)-trimethyl(4-(methylthio)pent-3-en-1-inyl)silane (**3f**) after column chromatography.

Hence, various alternative methylation sources were assessed. These experiments revealed that iodomethane (MeI) clearly outperforms the applied analogs (trifluoromethanesulfonate (MeOTf), dimethyl sulfate (Me_2SO_4) and methyl 4-methylbenzenesulfonate (MeOTs)) with regard to efficiency and selectivity. Further information on potential side reactions is given in chapter 2 in the Supplementary Data (acid-induced isomerization pathways).

As a consequence, the second approach was to avoid the formation of I_2. On the one hand, the removal of I^- with Ag^+-salts (e.g. Ag_2CO_3) and, on the other hand, the addition of a reducing agent were attempted for this purpose. In both cases, the formation of *E*-isomer was entirely suppressed. Particularly the application of Na_2SO_3 as the reducing agent prior to the addition of MeI proved to be advantageous. This new procedure for TRF, also applying slightly modified reaction parameters, combines both the prevention of the isomerization and the ease of workup. In addition to the significant improvement in stereospecificity an enhanced isolated yield of 86% (vs. 76–81% using the old procedure)[30] for **3a** was obtained, which shows the efficiency of the protocol.

To demonstrate the scope of the developed protocol, various substrates for TRF reactions were evaluated (Scheme 2). The modifications of **2a** include the introduction of more stable silyl groups R (from TMS to TBDMS and TIPS) and variation in the substituent R′ in the thiophene 5-position (from sp^3 to sp^2 and sp hybridization). The diversity of suitable silyl groups is an important factor with regard to specific functionalization. The alteration towards sp^2 and sp centers for R′ derives from the current interest in these compounds as organic functional π-systems (e.g. NLO materials).

Detailed synthetic protocols for the synthesis of precursors **2a-e** *via* Halogen-Dance reactions[36] and TRF towards **3a-e** are given in the experimental section. Applying the novel TRF protocol all ring-opening reactions were accomplished successfully and in good yields of 75–86% without any formation of *E*-isomer; the proof for the formation of the *Z*-isomers has been given by X-ray diffraction

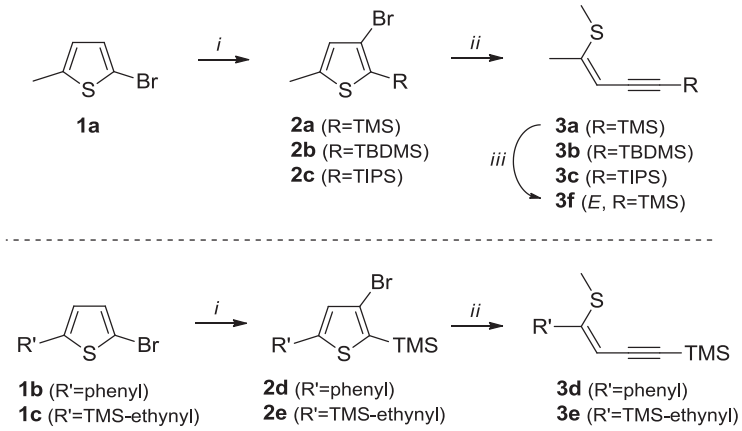

Scheme 2. Synthesis of compounds **3a-f**; *i*: HD-reaction; *ii*: new TRF-protocol; *iii*: I_2-induced isomerization.

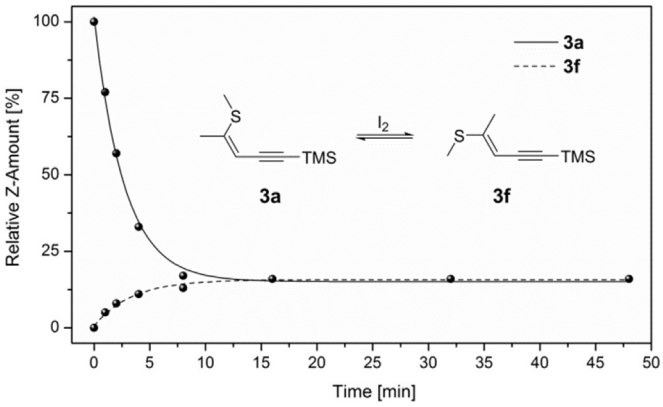

Fig. 1. I_2-induced isomerization of ene-yne compounds **3a** and **3f** (1.0 mol% I_2 solution in $CDCl_3$); curve fitting performed using standard exponential fit parameters.

on various examples.[37,38] A tendency towards lower yields for larger silyl groups (**3a**/**3b**/**3c** = 86%/82%/75%) and an increase in yields for sp to sp^2 and sp^3 hybridization of R' (**3e**/**3d**/**3a** = 77%/81%/86%) has been observed (see Table 1).

2.2. Kinetic investigations

Although the TRF reaction has been extensively studied regarding the substrate scope, no kinetic data is available. Based on previous investigations[39] on organo-lithium compounds an ATR-IR probe was applied for inline reaction monitoring to explore the ring-opening process under dynamic conditions in order to gain insight on fragmentation threshold temperatures and reaction kinetics. Recent progress in the development of mid-IR transparent fibres[40] and sensor assembly render it possible to achieve reliable data even under non-isothermal conditions. This allows for a monitoring of the TRF reaction in a warm-up phase yielding the onset temperature of the ring-opening. The inline approach (both *in-situ* and real-time) is of critical importance for this study, since alternative techniques typically suffer from sample alteration during sampling.[39]

In the initial experiments the fragmentation threshold temperatures were matter of interest. For this purpose the respective substrates (**2a**, **2b**, **2d**, **2e**) were lithiated *via* metal-halogen exchange using *n*-BuLi (1.1 eq.) at −60 °C in anhydrous Et_2O (0.2 M). The fragmentation of the TIPS-substituted derivative **2c** could not be monitored under the applied conditions due to the low solubility in Et_2O at −60 °C. After completion of the lithiation process the temperature was raised to ~0 °C at a constant rate (0.5 °C/min). Indeed, the formation of intense new absorption bands, particularly in the fingerprint region (650-900 cm^{-1}), were reproducibly observed for all substrates at certain temperatures. These bands reveal a significant correlation to peaks located between 2100 and 2200 cm^{-1} (highly specific for C–C triple bonds), which confirms the onset of the TRF reaction forming the ene-yne moiety. However, due to the self-absorption of the applied ATR-unit these bands were not utilized for quantitative analyses. The obtained concentration profiles during the ring-opening of **2a** are exemplarily depicted in Fig. 2 (profiles for all fragmentation products are given in the Supplementary Data). Remarkably, the obtained ring-opening temperatures (defined by a 5% intensity threshold relative to the baseline) are in contrast to literature values. Whereas thiophene ring-fragmentations are typically reported to occur at room-temperature,[1–3] we observed reaction on-set temperatures of −50 °C, −47 °C and −42 °C for **2a**, **2b** and **2e**, respectively. Only the fragmentation of **2d** was found to take place at higher temperature (−24 °C), which is attributed to stabilizing effects of the phenyl substituent (see Table 1).

Furthermore, we investigated the TRF of **2a** under isothermal conditions (−45 °C, −40 °C and −35 °C). A linear time dependence was observed for the product formation at all temperatures (Fig. 3) indicating a zero-order reaction, typically found for saturated catalytic processes. The reaction rates plotted against 1/T also show the linear dependence required by the Arrhenius equation, confirming this assumption (Supplementary Data). This finding is in obvious disagreement with the reaction mechanism depicted in Scheme 1, which implies a first-order reaction. To gain further insights we applied an excess *n*-BuLi and altered the concentration (0.13 M) of **2a**, however, did not find any significant influence of the variations on the reaction rate. At this point, the reason for the zero-

Table 1
Isolated yields and fragmentation temperatures of TRF products **3a-e**.

	Isolated Yield[a] [%]	TRF Temperature[b] [°C]
3a	86	−50
3b	82	−47
3c	75	n.o.[c]
3d	81	−24
3e	77	−42

[a] i) Et_2O (0.2 M), −40 °C, *n*-BuLi (1.1 eq.), ii) rt, 30 min, iii) −40 °C, Na_2SO_3 (1.2 eq.), iv) MeI (1.5 eq.), rt.
[b] Defined by 5% threshold temperature.
[c] Not observed due to low solubility.

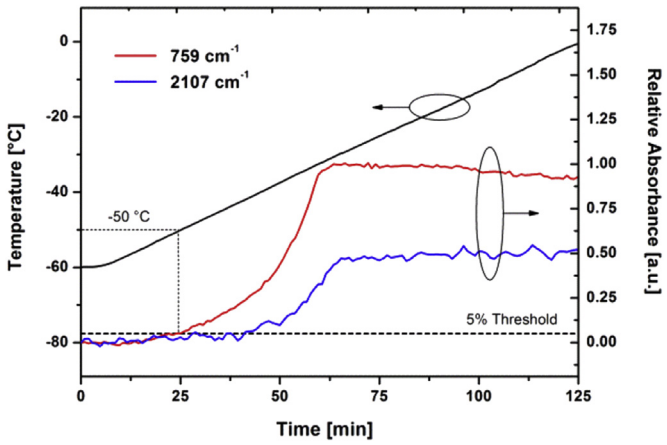

Fig. 2. Normalized integrals of selected absorption bands of **3a** and temperature gradient during TRF of **2a**.

order kinetics is not understood and remains to be clarified by future research.

2.3. Flow chemistry

Problems associated with solvent interactions, highly exothermic reactions and other safety issues limit the applicability of organolithium reagents to low temperature regimes. Unfortunately, the scale-up of cryogenic reactions employing hazardous reagents such as organometallic compounds under strictly inert conditions tend to be troublesome and error-prone. However, excellent heat transfer and short residence times (t^R) allow those reactions to be conducted safely in a microflow reactor. Inspired by previous reports on ring-fragmentation under flow conditions,[41] we therefore aimed to incorporate the TRF to an automated flow process, providing wide scalability and safe operation conditions. Furthermore, the application of such a microflow reactor guarantees fully inert atmosphere which is of crucial importance in order to avoid the formation of the undesired *E*-isomer. Low fragmentation temperatures observed during IR-experiments allow for short residence times in a microflow reactor under convenient temperature (Fig. 4).

A stainless steel microreactor was fabricated (Fig. 5), consisting of individual pre-cooling zones for reagents (200 μL volume each), T-shaped mixers and two microfluidic reaction zones – one for the lithiation (1 mL volume) and one for the quench (1.5 mL volume). In order to allow reaction temperatures down to −40 °C, a dual-stage Peltier-assisted cooling module was developed (FlowChiller), and attached to the bottom of the stainless steel reactor.

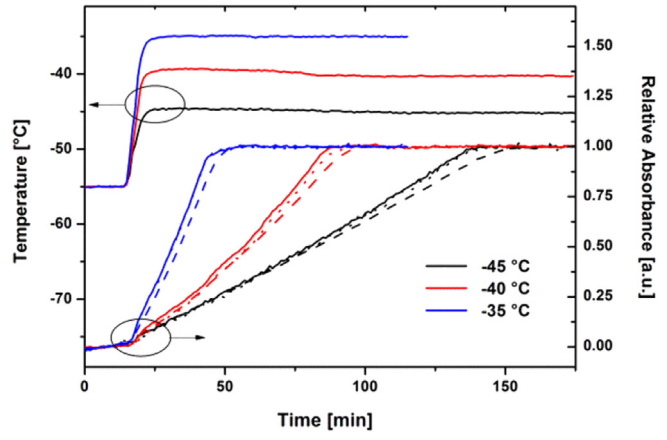

Fig. 3. Normalized integrals of absorption bands at 1249 cm^{-1} (solid), 854 cm^{-1} (dashed) and 759 cm^{-1} (dotted) of **3a** during TRF under isothermal conditions.

Precooled solutions of **2a** (1.0 eq., 0.1 mol L^{-1} in Et_2O) and *n*-BuLi (1.1 eq., 1.6 mol L^{-1} in hexanes) were mixed and lithiation as well as TRF was accomplished in the lithiation reactor. Subsequently, a solution of MeI (1.8 eq., 0.35 mol L^{-1} in Et_2O) was added and methylation of the thiolate took place in the quench-reactor. Finally, after leaving the microflow reactor, the reaction mixture was collected in a vial containing a Na_2SO_3 solution to avoid isomerization induced by atmospheric oxygen. Reaction temperature (−40 °C, −20 °C, 0 °C and room temperature) as well as t^R (5–60 s) in the lithiation reactor were varied in order to identify ideal reaction conditions. Overall recovery of product, starting material and dehalogenated starting materials was approximately 75–80% at room temperature and almost quantitative beneath −20 °C. While virtually no product formation was observed at −40 °C (as expected from kinetic data), low conversion (34% yield) towards **3a** took place at $t^R = 60$ s at −20 °C. Notably, in both experiments only small amounts of dehalogenated by-product were formed, while the majority of the recovered material was starting compound **2a** indicating that TRF proceeds rapidly compared to the initial lithiation in the investigated temperature regime. At 0 °C significantly increased product formation was observed for higher values of t^R, while best results were obtained at room temperature (Fig. 6). Fragmentation is basically completed after 20 s and the highest yield (73%) was found at $t^R = 30$ s. Remarkably, no formation of the *E*-isomer was observed in any of our experiments. Variation of t^R in the quench-reactor did not significantly influence the outcome of the experiment. More detailed results of the screening are given in Table S2 and S3 in the Supplementary Data.

Applying the optimized conditions, a run on a preparative scale (12 mmol, room temperature, $t^R = 60$ s) was conducted. After purification by column chromatography, **3a** could be obtained in 56% yield.

2.4. Non linear optical properties

Recently, we showed that replacing sulfur by selenium in ene-yne derived NLO-materials significantly boosts the SH-efficiency. This outcome can be attributed to increased density of delocalized electrons in the conjugated π-system and thus enhanced hyperpolarizibility.[31] However, the application of selenium is accompanied by drawbacks such as the toxicity of organo-selenium compounds and complex synthesis of the required precursors. We therefore adopted a novel design strategy to increase the electron-density in the conjugated π-system. By attaching electron-donating substituents to the phenyl subunit, the molecular architecture was extended to a donor-acceptor-donor structure as depicted in Scheme 3.

The syntheses of **5i-iii** were accomplished *via* CuAAC starting from **3a** and the corresponding azides **4i-iii** in moderate to good yields (**5i**: 82%, **5ii**: 34%, **5iii**: 57%). A fundamental prerequisite for SHG (second harmonic generation) is the crystallization in a non-centrosymmetric crystal class, with the exception of 432.[42] Unfortunately, **5ii**[43] and **5iii**[44] both crystallized in the centrosymmetric space group $P2_1/c$. In contrast, enantiomorphic crystals of **5i**[45] (space group $P2_1$, Flack parameter 0.00(2)) were grown by slow solvent evaporation (EtOH) > 25 °C. A second centrosymmetric polymorph of **5i**[46] (space group: $P2_1/c$) was obtained by growing crystals from a saturated EtOH solution upon cooling to ~ 5 °C.

The molecules in the $P2_1$ polymorph of **5i** ($Z' = 1$) crystallize in layers parallel to (001), whereby the molecules are significantly

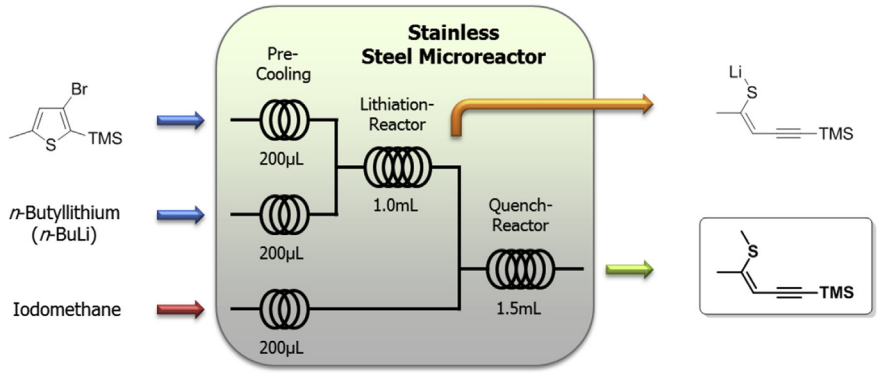

Fig. 4. Microreactor setup for continuous-flow experiments.

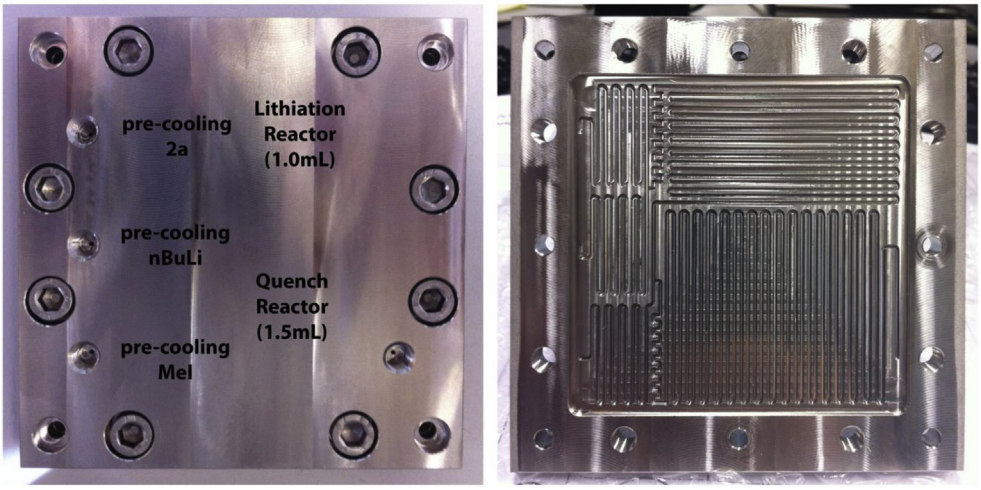

Fig. 5. Stainless steel microreactor equipped with pre-cooling zones, a lithiation reaction zone and a quench reaction zone.

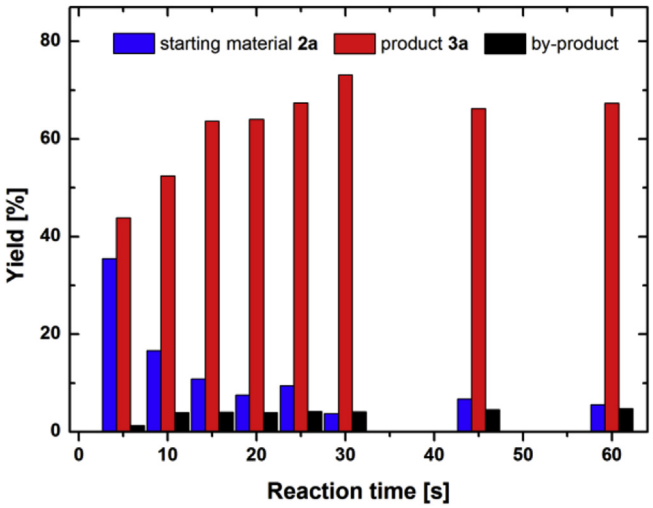

Fig. 6. Reaction course at room temperature and reaction times from 5 to 60 s.

inclined with respect to the stacking direction (Fig. 7). Inside these layers, molecules related by translation along **a** are connected *via* face-to-face contacts of benzene to triazole rings (distance of least squares planes defined by the benzene rings of two adjacent molecules 3.519 Å).

The $P2_1/c$ polymorph (Z' = 1) is crystallo-chemically unrelated to the $P2_1$ polymorph. The conformations of the molecules in both polymorphs differ regarding the orientation of the methoxy group and the molecule in the $P2_1$ polymorph is considerably more twisted: The least squares planes defined by the non-H atoms of the benzene ring and the triazole ring form an angle of 26.7°, while the benzene and CH=CS-CH_3-fragment form an angle of 18.9°. The analogous angles in the $P2_1/c$ polymorph are 9.0° and 8.7°.

Enantiomorphic crystals of **5i** were subjected to SHG measurements (Fig. 8). Compared to parent compound **I** (Scheme 3; R = H) **5i** (R = OMe) exhibits 35-fold increased SHG-efficiency or ~ 80-times the value of KDP (potassium dihydrogen phosphate). The nonlinear performance of **5i** is the highest reported for TRF-derived

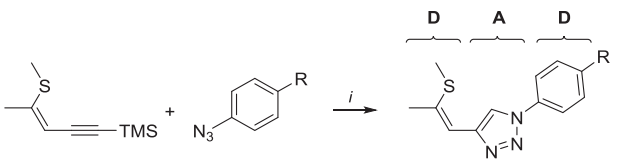

Scheme 3. Synthesis of "Click"-functionalized ene-yne derivatives **5i-iii** *via* CuAAC; *i*: $CuSO_4 \cdot 5H_2O$, Na ascorbate, KF; D = Electron Donor, A = Electron Acceptor.

NLO chromophores so far and underlines the efficiency of the proposed donor-acceptor-donor design.

3. Conclusion

Systematic investigations on the thiophene ring-fragmentation reaction focusing on improved selectivity as well as enhanced efficiency have been presented. The application of state of the art inline reaction monitoring technique revealed novel insights to fragmentation on-set temperatures and reaction kinetics. As a result, reliable synthetic procedures for lab-scale (Na_2SO_3 method) as well as mid- to large-scale (flow chemistry) were established. In addition a new design concept for ene-yne based NLO materials was developed, which strengthens the relevance of TRF products in the field of functional organic materials.

4. Experimental section

4.1. Synthesis

4.1.1. General procedures and methods

All reactions were performed in oven-dried glassware. Reagents were purchased from common commercial sources and used without prior purification. Anhydrous solvents were prepared by filtration through drying columns. Column chromatography was performed on silica 60 (40–63 μm) using distilled solvents as given. Melting points were recorded on an Automated Melting Point System and are corrected.

NMR spectra were recorded at 400 MHz for ^{1}H and 100 MHz for ^{13}C for all target compounds (ene-yne) and at 200 MHz for ^{1}H and 50 MHz for ^{13}C for intermediates. Data for ^{1}H NMR are reported as follows: chemical shift in parts per million (ppm) from TMS (tetramethylsilane) with the residual solvent signal as an internal reference ($CDCl_3$ δ = 7.26 ppm), multiplicity (s = singlet, d = doublet, t = triplet and m = multiplet), coupling constant in Hz and integration. ^{13}C NMR spectra are reported in ppm from TMS using the central peak of the solvent as reference ($CDCl_3$ δ = 77.0 ppm); multiplicity with respect to proton (deduced from APT experiments, s = quaternary C, d = CH, t = CH_2, q = CH_3).

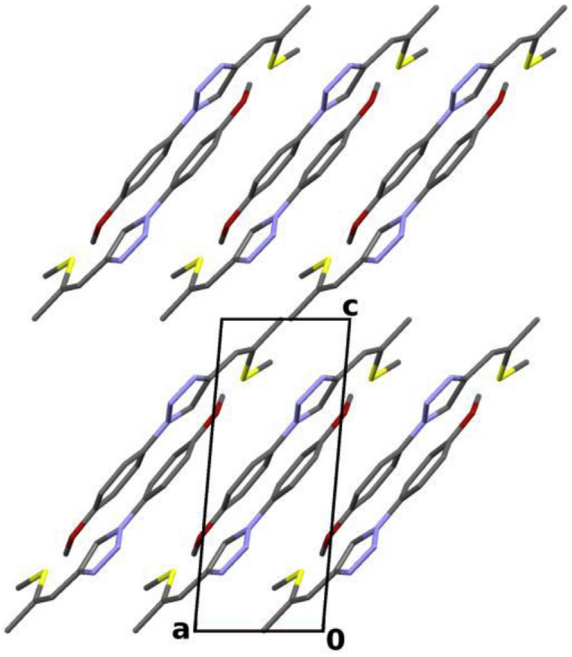

Fig. 7. The crystal structure of the $P2_1$ polymorph of **5i** viewed down [010]; C, N, O and S atoms are grey, blue, red and yellow, respectively; H atoms have been omitted for clarity.

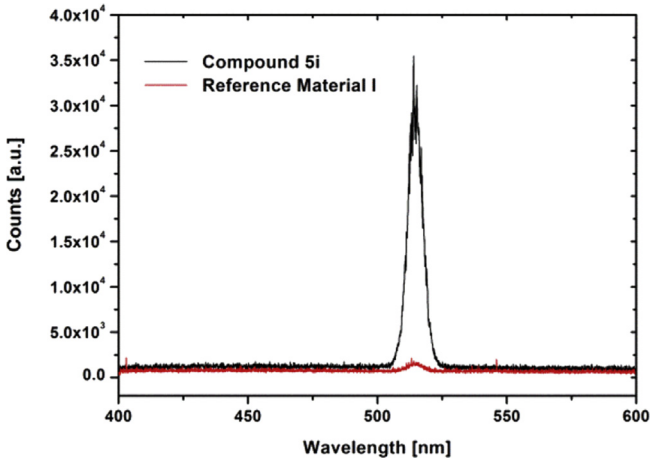

Fig. 8. SHG spectra of **5i** and reference material **I**; the lineshape is a replica of the emission spectrum of the femtosecond laser used in the experiment and shows the relatively large bandwidth typical for femtosecond lasers.

4.1.2. General procedure for the halogen dance (HD) reaction[36]

To a solution of diisopropylamine (DIPA, 1.4 eq.) in anhydrous THF under argon *n*-BuLi (1.2 eq.) was slowly added at −30 to −40 °C. After 30–60 min the thiophene species (**1**, 1.0 eq.) was added in anhydrous THF at −70 °C and the reaction stirred for 1.5–2 h. Subsequently, the appropriate silyl chloride (1.2 eq.) was added as a solution in anhydrous THF and the mixture stirred at rt overnight. The reaction was poured on water, extracted with Et_2O, the organic phases were dried over anhydrous Na_2SO_4 and concentrated under reduced pressure.

4.1.3. General procedure for the thiophene ring-fragmentation (TRF) reaction

To a solution of **2a-c** (1.0 eq.) in anhydrous Et_2O (~0.2 M) under argon atmosphere at −40 to −60 °C *n*-BuLi (1.1 eq.) was injected dropwise. After the addition the reaction was immediately warmed to rt, stirred for 30 min and again cooled to −40 °C. At this point the addition of first Na_2SO_3 (1.2 eq.) then MeI (1.5 eq.) was accomplished and the temperature subsequently raised to rt. After a reaction time of 20–60 min the mixture was poured on water, extracted with Et_2O, the combined organic layers were washed with brine, dried over anhydrous Na_2SO_4 and concentrated *in vacuo*. Purification was performed by column chromatography (light petroleum).

4.1.4. General procedure for CuAAC

To a suspension of **3a** (1.2 eq.), azide (1.0 eq.), Na ascorbate (0.4 eq.) and $CuSO_4 \cdot 5H_2O$ (0.2 eq.) in t-BuOH/H_2O (1:1, ~0.4 M) in a microwave reaction vial was added KF (1.4 eq.) at room temperature. Subsequently, the reaction vial was sealed and heated to 150 °C for 30 min in a reaction microwave. Then the reaction mixture was poured on H_2O and extracted with Et_2O. The combined organic layers were washed with brine, dried over anhydrous Na_2SO_4 and concentrated under reduced pressure. Final purification was accomplished by column chromatography.

4.1.5. Synthetic details

The syntheses of 2-bromo-5-methylthiophene (**1a**),[47] 2-bromo-5-phenylthiophene (**1b**),[48,49] 2-bromo-5-[2-(trimethylsilyl)

ethynyl]-thiophene (**1c**),[50,51] 3-bromo-5-methyl-2-(trimethylsilyl) thiophene (**2a**),[30] 1-azido-4-methoxybenzene (**4i**),[52] 1-azido-4-(methylthio)benzene (**4ii**)[52] and 4-azido-*N*,*N*-dimethylbenzenamine (**4iii**)[52] were performed according to published protocols.

4.1.6. 3-Bromo-2-[(1,1-dimethylethyl)dimethylsilyl]-5-methylthiophene (2b)

DIPA (5.20 g, 51.4 mmol) in anhydrous THF (150 mL), *n*-BuLi (18.0 mL, 45.0 mmol, 2.5 M in hexanes), **1a** (6.70 g, 37.8 mmol) in anhydrous THF (20 mL), TBDMS-Cl (15.0 mL, 45.0 mmol, 3 M in anhydrous THF) and purification by bulb-to-bulb distillation *in vacuo* yielded **2b** (8.07 g, 73%) as slightly yellow oil. BP: 73–74 °C (0.18 mbar). ^{1}H NMR (400 MHz, $CDCl_3$): $\delta = 6.78$ (s, 1H), 2.47 (s, 3H), 0.96 (s, 9H), 0.38 (s, 6H) ppm. ^{13}C NMR (100 MHz, $CDCl_3$): $\delta = 145.6$ (s), 131.1 (d), 130.1 (s), 117.0 (s), 26.8 (q), 18.2 (s), 15.1 (q), −4.3 (q) ppm. Anal. Calcd for $C_{11}H_{19}BrSSi$: C, 45.35; H, 6.57; *m/z* 290.02 $[M]^+$. Found: C, 45.58; H, 6.61; MS (EI, quadrupole): *m/z* 290.07 $[M]^+$.

4.1.7. 3-Bromo-2-[tris(1-methylethyl)silyl]-5-methylthiophene (2c)

DIPA (1.09 g, 10.8 mmol) in anhydrous THF (80 mL), *n*-BuLi (3.8 mL, 9.6 mmol, 2.5 M in hexanes), **1a** (1.41 g, 8.0 mmol) in anhydrous THF (20 mL), TIPS-Cl (1.85 g, 9.6 mmol) in anhydrous THF (15 mL) and purification by column chromatography (light petroleum) yielded **2c** (2.14 g, 80%) as white solid. MP: 48.4–49.5 °C. ^{1}H NMR (400 MHz, $CDCl_3$): $\delta = 6.79$ (s, 1H), 2.48 (s, 3H), 1.55 (sept., $J = 7.5$ Hz, 3H), 1.13 (d, $J = 7.5$ Hz, 18H) ppm. ^{13}C NMR (100 MHz, $CDCl_3$): $\delta = 145.5$ (s), 131.2 (d), 128.0 (s), 116.9 (s), 18.8 (q), 15.1 (q), 12.4 (d) ppm. Anal. Calcd for $C_{14}H_{25}BrSSi$: C, 50.43; H, 7.56; *m/z* 332.06 $[M]^+$. Found: C, 50.64; H, 7.65; MS (EI, quadrupole): *m/z* 332.06 $[M]^+$.

4.1.8. 3-Bromo-5-phenyl-2-(trimethylsilyl)thiophene (2d).[53]

DIPA (6.86 g, 67.8 mmol) in anhydrous THF (160 mL), *n*-BuLi (24.1 mL, 60.2 mmol, 2.5 M in hexanes), **1b** (12.0 g, 50.2 mmol) in anhydrous THF (40 mL) were mixed as described in the general procedure and stirred for 2 h at 40 °C. After the addition of TMS-Cl (6.54 g, 60.2 mmol) in anhydrous THF (60 mL) and purification by bulb-to-bulb distillation under reduced pressure **2d** (14.76 g, 94%) was isolated as colorless oil. BP: ~110 °C (0.05 mbar). Physical properties in agreement with literature.[53]

4.1.9. 3-Bromo-2-(trimethylsilyl)-5-[2-(trimethylsilyl)ethynyl] thiophene (2e)

Alterations to the general procedure. A precooled (−40 °C) solution of LDA (DIPA (0.49 g, 4.8 mmol), *n*-BuLi (1.9 mL, 4.6 mmol, 2.4 M in hexanes, anhydrous THF (40 mL)) was added to as stirred suspension of **1c** (1.00 g, 3.9 mmol) in anhydrous THF (40 mL) at −35 °C under argon atmosphere. After a reaction time of 30 min TMS-Cl (0.60 g, 5.6 mmol) in anhydrous THF (5 mL) was injected rapidly and the mixture warmed to rt. Standard work-up (general procedure) and column chromatography (light petroleum) gave **2e** (0.84 g, 66%) as slightly yellow oil. BP: ~111 °C (0.2 mbar). ^{1}H NMR (400 MHz, $CDCl_3$): $\delta = 7.17$ (s, 1H), 0.38 (s, 9H), 0.23 (s, 9H) ppm. ^{13}C NMR (100 MHz, $CDCl_3$): $\delta = 137.6$ (s), 136.7 (d), 128.3 (s), 116.1 (s), 101.3 (s), 95.9 (s), −0.3 (q), −0.9 (q) ppm. Anal. Calcd for $C_{12}H_{19}BrSSi_2$: C, 43.49; H, 5.78; *m/z* 329.99 $[M]^+$. Found: C, 43.87; H, 5.47; MS (EI, quadrupole): *m/z* 329.96 $[M]^+$.

4.1.10. Trimethyl[(3Z)-4-(methylthio)-3-penten-1-yn-1-yl]silane 3a

Starting from **2a** (2.98 g, 12.0 mmol), *n*-BuLi (5.3 mL, 13.2 mmol, 2.5 M in hexanes), Na_2SO_3 (1.81 g, 14.4 mmol) and MeI (2.55 g, 18.0 mmol) pure *Z*-isomer **3a** (1.90 g, 86%) was isolated as a colorless to slightly yellow liquid after a reaction time of 20 min at rt subsequent to the addition of the methyl-species. Physical data is in accordance to published values.[30]

4.1.11. (1,1-Dimethylethyl)dimethyl[(3Z)-4-(methylthio)-3-penten-1-yn-1-yl]silane 3b

Starting from **2b** (583 mg, 2.0 mmol), *n*-BuLi (0.9 mL, 2.2 mmol, 2.5 M in hexanes), Na_2SO_3 (303 mg, 2.4 mmol) and MeI (426 mg, 3.0 mmol) **3b** (370 mg, 82%) was isolated as a yellow low melting solid after a reaction time of 60 min at rt after the addition of MeI. ^{1}H NMR (400 MHz, $CDCl_3$): $\delta = 5.43$ (s, 1H), 2.36 (s, 3H), 2.07 (s, 3H), 0.97 (s, 9H), 0.13 (s, 6H) ppm. ^{13}C NMR (100 MHz, $CDCl_3$): $\delta = 149.4$ (s), 102.9 (d), 102.3 (s), 99.5 (s), 26.1 (q), 22.3 (q), 16.6 (s), 14.0 (q), −4.5 (q) ppm. Anal. Calcd for $C_{12}H_{22}SSi$: *m/z* 227.1284 $[M + H]^+$. Found: MS (APCI, TOF): *m/z* 227.1281 $[M + H]^+$.

4.1.12. Tris(1-methylethyl)[(3Z)-4-(methylthio)-3-penten-1-yn-1-yl]silane 3c

Starting from **2c** (500 mg, 1.5 mmol), *n*-BuLi (0.65 mL, 1.7 mmol, 2.5 M in hexanes), Na_2SO_3 (227 mg, 1.8 mmol) and MeI (319 mg, 2.3 mmol) **3c** (302 mg, 75%) was isolated as colorless low melting solid after a reaction time of 60 min at rt subsequently to the addition of the methyl-species. ^{1}H NMR (400 MHz, $CDCl_3$): $\delta = 5.46$ (s, 1H), 2.36 (s, 3H), 2.08 (s, 3H), 1.10 (m, 21H) ppm. ^{13}C NMR (100 MHz, $CDCl_3$): $\delta = 149.0$ (s), 103.4 (s), 103.2 (d), 97.6 (s), 22.2 (q), 18.7 (q), 14.0 (q), 11.3 (d) ppm. Anal. Calcd for $C_{15}H_{28}SSi$: *m/z* 269.1754 $[M + H]^+$. Found: MS (APCI, TOF): *m/z* 269.1746 $[M + H]^+$.

4.1.13. Trimethyl[(3Z)-4-(methylthio)-4-phenyl-3-buten-1-yn-1-yl] silane 3d

Starting from **2d** (623 mg, 2.0 mmol), *n*-BuLi (0.9 mL, 2.2 mmol, 2.5 M in hexanes), Na_2SO_3 (303 mg, 2.4 mmol) and MeI (426 mg, 3.0 mmol) **3d** (397 mg, 81%) was isolated as yellow oil after a reaction time of 30 min at rt after the addition of MeI. ^{1}H NMR (400 MHz, $CDCl_3$): $\delta = 7.41$–7.33 (m, 5H), 5.76 (s, 1H), 2.13 (s, 3H),0.26 (s, 9H) ppm. ^{13}C NMR (100 MHz, $CDCl_3$): $\delta = 152.6$ (s), 138.2 (s), 128.7 (d), 128.5 (d), 128.0 (d), 107.5 (d), 103.2. (s), 102.2 (s), 16.1 (q), 0.0 (q) ppm. Anal. Calcd for $C_{14}H_{18}SSi$: *m/z* 247.0971 $[M + H]^+$. Found: MS (ESI, TOF): *m/z* 247.0958 $[M + H]^+$.

4.1.14. [(3Z)-3-(Methylthio)-3-hexen-1,5-diyn-1,6-diyl] bis(trimethylsilane) 3e

Starting from **2e** (331 mg, 1.0 mmol), *n*-BuLi (0.45 mL, 1.1 mmol, 2.5 M in hexanes), Na_2SO_3 (151 mg, 1.2 mmol) and MeI (213 mg, 1.5 mmol) **3e** (206 mg, 77%) was obtained as slightly orange low-melting solid after a reaction time of 30 min at rt subsequently to the addition of MeI. ^{1}H NMR (400 MHz, $CDCl_3$): $\delta = 5.87$ (s, 1H), 2.42 (s, 3H),0.22 (m, 18H) ppm. ^{13}C NMR (100 MHz, $CDCl_3$): $\delta = 133.9$ (s), 111.3 (d), 109.1 (s), 104.1 (s), 100.9 (s), 99.4 (s), 15.7. (q), −0.1 (q), −0.2 (q) ppm. Anal. Calcd for $C_{13}H_{22}SSi_2$: *m/z* 267.1054 $[M + H]^+$. Found: MS (ESI, TOF): *m/z* 267.1045 $[M + H]^+$.

4.1.15. Isomerization procedure towards trimethyl[(3E)-4-(methylthio)-3-penten-1-yn-1-yl]silane 3f

3a (220 mg, 1.2 mmol, 1.0 eq.) was dissolved in a solution of I_2 (12 μmol, 1.0 mol%) in $CHCl_3$ (~7 mL) in NMR glass tubes and irradiated with an external light source for 20 min (IntelliRay 600, 50% intensity) resulting in a relative *E*-isomer content of 86%. Subsequently, the mixture was diluted with $CHCl_3$ and extracted with an aqueous Na_2SO_3 solution. The organic layer was dried over anhydrous Na_2SO_4 and the solvent removed under reduced pressure. Column chromatography (light petroleum) yielded compound **3f** (167 mg, 76%) as slightly yellow oil. ^{1}H NMR (400 MHz, $CDCl_3$): $\delta = 5.12$ (s, 1H), 2.25 (s, 3H), 2.14 (s, 3H), 0.19 (s, 9H) ppm. ^{13}C NMR (100 MHz, $CDCl_3$): $\delta = 150.9$ (s), 102.5 (s), 99.0 (d), 97.7 (s), 20.6 (q), 14.7 (q), 0.1 (q) ppm. Anal. Calcd for $C_9H_{16}SSi$: *m/z* 185.0815 $[M + H]^+$. Found: MS (APCI, TOF): *m/z* 185.0810 $[M + H]^+$.

4.1.16. 4-[(1Z)-2-(Methylthio)-1-propen-1-yl]-1-(4-methoxyphenyl)-1H-1,2,3-triazol 5i

Starting from **3a** (1.55 g, 8.4 mmol), **4i** (1.04 g, 7.0 mmol), Na ascorbate (0.56 g, 2.8 mmol), $CuSO_4 \cdot 5H_2O$ (0.35 g, 1.4 mmol) and KF (0.57 g, 9.8 mmol) **5i** (1.50 g, 82%) was obtained after column chromatography (light petroleum/Et_2O 1:1). ^{1}H NMR (400 MHz, CD_2Cl_2): $\delta = 8.31$ (s, 1H), 7.66 (d, $J = 9.0$ Hz, 2H), 7.04 (d, $J = 9.0$ Hz, 2H), 6.61 (d, $J = 1.1$ Hz, 1H), 3.86 (s, 3H), 2.42 (s, 3H), 2.27 (d, $J = 1.1$ Hz, 3H) ppm. ^{13}C NMR (100 MHz, CD_2Cl_2): $\delta = 160.3$ (s), 145.6 (s), 135.9 (s), 131.2 (s), 122.6 (d), 120.6 (d), 115.2 (d), 115.1 (d), 56.2 (q), 23.8 (q), 14.7 (q) ppm. Anal. Calcd for $C_{13}H_{15}N_3OS$: *m/z* 262.1009 $[M + H]^+$. Found: MS (ESI, TOF): *m/z* 262.1010 $[M + H]^+$.

4.1.17. 4-[(1Z)-2-(Methylthio)-1-propen-1-yl]-1-[(4-methylthio) phenyl)]-1H-1,2,3-triazol 5ii

Starting from **3a** (288 mg, 1.56 mmol), **4ii** (215 mg, 1.30 mmol), Na ascorbate (103 mg, 0.52 mmol), $CuSO_4 \cdot 5H_2O$ (65 mg, 0.26 mmol) and KF (106 mg, 1.82 mmol) **5ii** (121 mg, 34%) was obtained after column chromatography (light petroleum/Et_2O 3:2). ^{1}H NMR (400 MHz, CD_2Cl_2): $\delta = 8.35$ (s, 1H), 7.69 (d, $J = 8.6$ Hz, 2H), 7.39 (d, $J = 8.6$ Hz, 2H), 6.62 (s, 1H), 2.54 (s, 3H), 2.42 (s, 3H), 2.27 (s, 3H) ppm. ^{13}C NMR (100 MHz, CD_2Cl_2): $\delta = 145.7, 140.2, 136.3, 134.8$, 127.6, 121.3, 120.4, 114.9, 23.8, 16.0, 14.7 ppm. Anal. Calcd for $C_{13}H_{15}N_3S_2$: *m/z* 278.0780 $[M + H]^+$. Found: MS (ESI, TOF): *m/z* 278.0783 $[M + H]^+$.

4.1.18. N,N-dimethyl-4-[4-[(1Z)-2-(methylthio)-1-propen-1-yl]-1H-1,2,3-triazol-1-yl]benzenamine 5iii

Starting from **3a** (288 mg, 1.56 mmol), **4iii** (211 mg, 1.30 mmol), Na ascorbate (103 mg, 0.52 mmol), $CuSO_4 \cdot 5H_2O$ (65 mg, 0.26 mmol) and KF (106 mg, 1.82 mmol) **5iii** (203 mg, 57%) was obtained after column chromatography (light petroleum/Et_2O 3:2). ^{1}H NMR (400 MHz, CD_2Cl_2): $\delta = 8.26$ (s, 1H), 7.56 (d, $J = 9.0$ Hz, 2H), 6.79 (d, $J = 9.0$ Hz, 2H), 6.61 (s, 1H), 3.01 (s, 6H), 2.41 (s, 3H), 2.26 (s, 3H) ppm. ^{13}C NMR (100 MHz, CD_2Cl_2): $\delta = 151.1$ (s), 145.3 (s), 135.4 (s), 127.3 (s), 122.2 (d), 120.5 (d), 115.4 (d), 112.7 (d), 40.8 (q), 23.8 (q), 14.7 (q) ppm. Anal. Calcd for $C_{14}H_{18}N_4S$: *m/z* 275.1325 $[M + H]^+$. Found: MS (ESI, TOF): *m/z* 275.1323 $[M + H]^+$.

4.2. IR monitoring

The ATR-IR fibre system consisted of a ReactIRTM 15 spectrometer equipped with an MCT (mercury cadmium telluride) detector (Mettler Toledo) connected to a DiComp Probe (Mettler Toledo, dimensions: 6.3 mm DSub AgX DiComp, 8 inches (203 mm) wetted length with a 1.5 m total length of AgX fiberconduit, optical window: 2500 to 650 cm^{-1}, temperature range: −80–180 °C, pH range: 1–14, wetted materials: alloy C276, diamond, gold). Spectra were recorded over the duration of the entire reaction at a spectral resolution of 4 cm^{-1}, averaging 76 scans yielding a temporal resolution of 30 s. The fibre probe was integrated in a double-walled cooling reactor (~10 mL volume) *via* feed-trough equipped with an argon inlet and a septum. The reaction vessel was charged with anhydrous solvent (Et_2O) and cooled by cryostat (Julabo) to −60 °C. After a steady temperature in the reactor was reached the background spectrum was recorded, the measurement started and the lithium species added. Subsequently the respective reactant was rapidly added *via* a syringe (concentrations and equivalents identical to the preparative experiments).

4.3. Flow chemistry

Screening experiments in the flow were carried out using three New Era NE-1000 syringe pumps. **2a** (4.98 g, 20.0 mmol) and *n*-dodecane (1.25 g) were dissolved in anhydrous Et_2O (200 mL) and a 50 mL (60 mL) syringe was filled with the solution. Methyl iodide (4.82 g, 33.9 mmol) was dissolved in anhydrous Et_2O (100 mL) and a 20 mL (24 mL) syringe was filled with the solution. A 10 mL syringe was filled with *n*-butyllithium (1.6 mol/L in hexanes). Na_2SO_3 (3.16 g, 25 mmol) was dissolved in deionized water (100 mL) and sixteen screw-cap vials were charged with Na_2SO_3 solution (1.35 mL each). The syringes were connected to the reactor inlets *via* Luer-Slip adapters as follows: starting material to inlet 1; *n*-butyllithium to inlet 2 and MeI to inlet 3. The chip reactor was placed on the FlowChiller[54] and the temperature was monitored. The outlet tube was placed in a waste bottle. Then 2 mL of every solution were pushed into the system. The desired flow rates were entered into the pumps. After starting the pumps, the dead volume time was awaited. Then the outlet tube was placed in the first vial and two subsequent samples were collected. Upon completion the vial was screwed tight and shaken vigorously. In such manner four sets of experiments were conducted at room temperature, 0 °C, −20 °C and −40 °C. Preparation of the vials and sample collection was conducted as described above. For GC analysis 256 μL of organic layer from every sample were transferred to a GC vial, diluted with 744 μL ethyl acetate, and analyzed. For the prep-scale experiment, reagents were prepared in the same way, whereas the syringe pumps were replaced with continuous pumps (Syrris Africa) and the reaction time was prolonged. After separation of the layers the diethyl ether was evaporated under reduced pressure. Purification of the crude product was accomplished *via* column chromatography (MPLC, light petrol, then ethyl acetate), yielding 1.258 g (56%) of pure product **3a** as a yellowish oil.

4.4. X-ray diffraction

Diffraction data of single crystals of **5i** (two polymorphs), **5ii** and **5iii** were collected on a Bruker KAPPA APEX II diffractometer system equipped with a CCD detector at 100 K under a dry stream of nitrogen using fine sliced ϕ- and ω-scans.[55] Data were reduced using SAINT-Plus[55] and corrected for absorption using SADABS.[55] The structures were solved with charge-flipping implemented in SUPERFLIP[56] and refined against *F* using Jana2006.[57] All non-H atoms were refined with anisotropic atomic displacement parameters. H atoms were located in difference Fourier maps and refined freely in **5i** (both polymorphs) and **5iii**. In **5ii** the H atoms were placed at calculated positions and refined as riding on the parent C atom.

4.5. Second harmonic generation

The second order nonlinear optical properties of the substances were screened with second harmonic measurements from powder samples, produced by grinding the sample crystals with a mortar to a particle size below <1 μm. A relative measurement of the nonlinear optical coefficients is possible with this technique since the SH efficiency scales quadratically with the nonlinear coefficient in this particle size regime.[58] The powder samples, sandwiched between microscope slides, were irradiated with the output of an ultrafast Yb:KGW-Laser (Light Conversion, pulse duration 70 fs, average power 600 mW, repetition rate 75 MHz, wavelength 1034 nm), moderately focused with a 100 mm focusing lens. The diffusely reflected SH-radiation was collected with a NA = 0.1 lens, separated from fundamental radiation with a color filter, and spectrally analyzed with a 0.25 m grating monochromator and a photomultiplier detector. The sample plane was positioned somewhat out of the focal plane (towards the lens) so as to prevent any damage to the sample. After each measurement, the samples were carefully checked for the absence of damage or thermal modification.

Acknowledgment

This work was supported in part by the TU Wien "Innovative Projects" research funds and the Austrian Federal Ministry of Science, Research and Economy. The authors acknowledge M. Lunzer, D. Wurm, D. Koch, B. Pokorny, D. Möstl, F. Krenn and A. Kempf for supporting the synthetic experiments. The authors also thank W. Skranc for preliminary work on this topic. N. Jankowski is acknowledged for conducting the ion chromatography and E. Rosenberg for performing the high resolution mass spectrometry (HRMS). The X-ray centre of the TU Wien is acknowledged for providing access to the single-crystal diffractometer.

Appendix A. Supplementary data

Supplementary data related to this article can be found at http://dx.doi.org/10.1016/j.tet.2016.12.025.

References

1. Gronowitz S, Frejd T. *Chem Heterocycl Compd*. 1978;14:353–367.
2. Iddon B. *Heterocycles*. 1983;20:1127–1171.
3. Gilchrist TL. In: Alan RK, ed. *Advances in Heterocyclic Chemistry*. Academic Press; 1987:41–74.
4. Moses P, Gronowitz S. *Arkiv Kemi*. 1961;18:119–132.
5. Gronowit S, Frejd T. *Acta Chem Scand*. 1969;23:2540–2542.
6. Gronowit S, Frejd P. *Acta Chem Scand*. 1970;24:2656–2658.
7. Jakobsen HJ. *Acta Chem Scand*. 1970;24:2663–2664.
8. Dickinson RP, Iddon B. *Tetrahedron Lett*. 1970:975–978.
9. Fuller LS, Iddon B, Smith KA. *Chem Commun*. 1997:2355–2356.
10. Fuller LS, Iddon B, Smith KA. *J Chem Society-Perkin Trans*. 1999;1:1273–1277.
11. Bobrovsky R, Hametner C, Kalt W, Fröhlich J. *Heterocycles*. 2008;76:1249–1259.
12. Santana AS, Carvalho DB, Casemiro NS, et al. *Tetrahedron Lett*. 2012;53:5733–5738.
13. Arisawa M, Igarashi Y, Tagami Y, Yamaguchi M, Kabuto C. *Tetrahedron Lett*. 2011;52:920–922.
14. Alves D, Sachini M, Jacob RG, et al. *Tetrahedron Lett*. 2011;52:133–135.
15. Xu H, Gu SJ, Chen WZ, Li DC, Dou JM. *J Org Chem*. 2011;76:2448–2458.
16. Dabdoub MJ, Dabdoub VB, Lenardao EJ, et al. *Synlett*. 2009:986–990.
17. Murai T, Fukushima K, Mutoh Y. *Org Lett*. 2007;9:5295–5298.
18. Skranc, W., reportPhD Thesis, TU Wien, 1999.
19. Bohlmann F, Haffer G. *Chem Berichte*. 1969;102:4017–4024.
20. Glöcklhofer F, Lumpi D, Kohlstädt M, Yurchenko O, Würfel U, Fröhlich J. *React Funct Polym*. 2015;86:16–26.
21. Bohlmann F, Skuballa W. *Chem Berichte*. 1970;103:1886–1893.
22. Bohlmann F, Burkhardt T, Zdero C. *Naturally Occurring Acetylenes*. London, New York: Academic Press; 1973.
23. Karlsson JO, Gronowitz S, Frejd T. *J Org Chem*. 1982;47:374–377.
24. Lam HW, Cooke PA, Pattenden G, Bandaranayake WM, Wickramasinghe WA. *J Chem Society-Perkin Trans*. 1999;1:847–848.
25. Marcantoni E, Massaccesi M, Petrini M, et al. *J Org Chem*. 2000;65:4553–4559.
26. Kuligowski C, Bezzenine-Lafollee S, Chaume G, et al. *J Org Chem*. 2002;67:4565–4568.
27. Liu G, Huth JR, Olejniczak ET, et al. *J Med Chem*. 2001;44:1202–1210.
28. Nielsen SF, Nielsen EO, Olsen GM, Liljefors T, Peters D. *J Med Chem*. 2000;43:2217–2226.
29. Lumpi D, Horkel E, Stoeger B, et al. Novel ene-yne compounds as quadratic nonlinear optical materials. In: *Proc. SPIE*. Photonics, Devices, and Systems V. vol. 8306. October 11, 2011:830615. http://dx.doi.org/10.1117/12.912457.
30. Lumpi D, Stöger B, Hametner C, et al. *CrystEngComm*. 2011;13:7194–7197.
31. Lumpi D, Glöcklhofer F, Holzer B, et al. *Cryst Growth & Des*. 2014;14:1018–1031.
32. Tornoe CW, Christensen C, Meldal M. *J Org Chem*. 2002;67:3057–3064.
33. Rostovtsev VV, Green LG, Fokin VV, Sharpless KB. *Angew Chem Int Ed*. 2002;41:2596–2599.
34. Moussebo C, Dale J. *J Chem Soc C Org*. 1966:260–264.
35. NMR tubes (Schott Duran), CDCl3 (Euriso-Top), standard light source (IntelliRay 600, Uvitron International, 600 W metal halide type lamp, intensity level 50 %). Prior to the experiment $CDCl_3$ was extracted with saturated aqueous $NaHCO_3$ solution and dried over molecular sieve to prevent side effects from acidic residues.
36. Fröhlich J, Hametner C, Kalt W. *Monatsh für Chem/Chem Mon*. 1996;127:325–330.
37. Lumpi D, Kautny P, Stöger B, Fröhlich J. *IUCrJ*. 2015;2:584–600.
38. Lumpi D, Kautny P, Stöger B, Fröhlich J. *Acta Crystallogr, Sect B Struct Sci, Cryst Eng Mater*. 2016;72:753–762.
39. Lumpi D, Wagner C, Schöpf M, et al. *Chem Commun*. 2012;48:2451–2453.
40. Harrington JA. *Handbook of Optics*. 3 ed. The McGraw-Hill Companies; 2010.
41. Asai T, Takata A, Ushiogi Y, Iinuma Y, Nagaki A, Yoshida J. *Chem Lett*. 2011;40:393–395.
42. Klapper H, Hahn T. In: Hahn T, ed. *International Tables for Crystallography*. Dordrecht: Springer; 2005:804.
43. 5ii): $C_{13}H_{15}N_3S_2$, M_r = 277.4, monoclinic, $P2_1/c$, a = 12.1159(4) Å, b = 14.6389(9) Å, c = 7.6543(7) Å, β = 107.959(4)°, V = 1291.44(15) Å^3, Z = 4, μ = 0.397 mm^{-1}, T = 100 K, 15795 measured, 2924 independent and 1738 observed [$I > 3\sigma(I)$] reflections, 164 parameters, wR (all data) = 0.0658, R [$I > 3\sigma(I)$] = 0.0509; CCDC reference number 1453300.
44. 5iii): $C_{14}H_{18}N_4S$, M_r = 274.4, monoclinic, $P2_1/c$, a = 11.0084(2) Å, b = 8.08390(10) Å, c = 15.7948(3) Å, β = 105.7583(8)°, V = 1352.76(4) Å^3, Z = 4, μ = 0.231 mm^{-1}, T = 100 K, 53619 measured, 4901 independent and 3986 observed [$I > 3\sigma(I)$] reflections, 244 parameters, wR (all data) = 0.0454, R [$I > 3\sigma(I)$] = 0.0345; CCDC reference number 1453301.
45. (5i), polymorph I: $C_{13}H_{15}N_3OS$, M_r = 261.3, monoclinic, $P2_1$, a = 4.6978(3) Å, b = 11.8173(8) Å, c = 11.4978(8) Å, β = 94.974(3)°, V = 635.90(7) Å^3, Z = 2, μ = 0.246 mm^{-1}, T = 100 K, 39787 measured, 7967 independent and 7364 observed [$I > 3\sigma(I)$] reflections, 223 parameters, wR (all data) = 0.0288, R [$I > 3\sigma(I)$] = 0.0252, Flack parameter 0.00(2); CCDC reference number 1453298.
46. (5i), polymorph II: $C_{13}H_{15}N_3OS$, M_r = 261.3, monoclinic, $P2_1/c$, a = 12.5889(5) Å, b = 9.1066(4) Å, c = 11.0679(5) Å, β = 94.6707(16)°, V = 1264.63(9) Å^3, Z = 4, μ = 0.247 mm^{-1}, T = 100 K, 53752 measured, 4634 independent and 4163 observed [$I > 3\sigma(I)$] reflections, 223 parameters, wR (all data) = 0.0493, R [$I > 3\sigma(I)$] = 0.0300; CCDC reference number 1453299.
47. Nakayama J, Konishi T, Murabayashi S, Hoshino M. *Heterocycles*. 1987;26:1793–1796.
48. Vachal P, Toth LM. *Tetrahedron Lett*. 2004;45:7157–7161.
49. Goldberg Y, Alper H. *J Org Chem*. 1993;58:3072–3075.
50. Skranc, W., Diploma Thesis, TU Wien, 1996.
51. Huang C, Zhen CG, Su SP, Loh KP, Chen ZK. *Org Lett*. 2005;7:391–394.
52. Grimes KD, Gupte A, Aldrich CC. *Synthesis Stuttgart*. 2010:1441–1448.
53. Kobatake S, Imagawa H, Nakatani H, Nakashima S. *New J Chem*. 2009;33:1362–1367.
54. M. Schoen, M. D. Mihovilivic, M. Schnuerch PCT Int. Appl., 2013, WO 2013006878 A1 20130117.
55. Bruker Analytical X-ray Instruments, Inc., Madinson, WI, USA: SAINT and SADABS 2008.
56. Palatinus L, Chapuis G. *J Appl Crystallogr*. 2007;40:786–790.
57. Petricek V, Dusek M, Palatinus L. *Z Krist – Cryst Mater*. 2014;229:345–352.
58. Kurtz SK, Perry TT. *J Appl Phys*. 1968;39:3798–3813.